Multiscale Analysis of Microvascular Blood Flow: A Multiscale Entropy Study of Laser Doppler Flowmetry Time Series

Anne Humeau*, Guillaume Mahé, François Chapeau-Blondeau, David Rousseau, and Pierre Abraham

***Abstract*—Processes regulating the cardiovascular system (CVS) are numerous. Each possesses several temporal scales. Their interactions lead to interdependences across multiple scales. For the CVS analysis, different multiscale studies have been proposed, mostly performed on heart rate variability signals (HRV) reflecting the central CVS; only few were dedicated to data from the peripheral CVS, such as laser Doppler flowmetry (LDF) signals. Very recently, a study implemented the first computation of multiscale entropy for LDF signals. A nonmonotonic evolution of multiscale entropy with two distinctive scales was reported, leading to a markedly different behavior from the one of HRV. Our goal herein is to confirm these results and to go forward in the investigations on origins of this behavior. For this purpose, 12 LDF signals recorded simultaneously on the two forearms of six healthy subjects are processed. This is performed before and after application of physiological scales-based filters aiming at isolating previously found frequency bands linked to physiological activities. The results obtained with signals recorded simultaneously on two different sites of each subject show a probable central origin for the nonmonotonic behavior. The filtering results lead to the suggestion that origins of the distinctive scales could be dominated by the cardiac activity.**

***Index Terms*—Laser Doppler flowmetry (LDF), microvascular blood flow, multiscale analysis, multiscale entropy.**

I. Introduction

THE CARDIOVASCULAR system (CVS) is regulated by multiple processes. Each of these processes has its own temporal scales and their interactions lead to a multiscale behavior for the CVS. This is true both for the central and the peripheral CVSs. The central CVS corresponds to the activities at the heart itself and can be analyzed with heart rate variability (HRV) data. The peripheral CVS can be studied through laser Doppler flowmetry (LDF) time series [1], [2]. LDF signals correspond to the microvascular blood flow and are commonly used in clinical research to monitor the microvascular function that controls the peripheral resistances. LDF signals exhibit complex fluctuations (see Fig. 1) that have been the subject of many recent studies to understand their underlying biophysical origins (see, e.g., [3]–[5]).

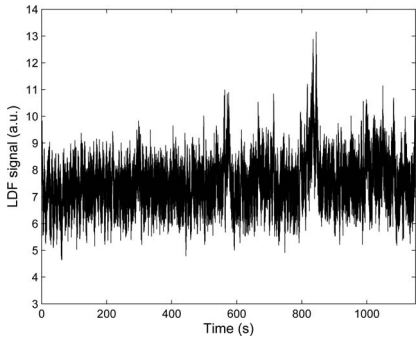

Fig. 1. LDF signal recorded on the forearm of a healthy subject. The sampling period T is 0.05 s and the acquisition duration is 19.16 min.

Different multiscale studies have been performed on data from the central CVS (HRV data). Some of them used a multifractal analysis, others a scale-dependent Lyapunov exponents study (see, for example, [6]–[8]). Recently, some authors have proposed a multiscale entropy analysis of HRV data [9], [10]. Multiscale entropy aims at quantifying irregularity of processes taking into account their multiple time scales. It has been shown that multiscale entropy of HRV data is able to separate healthy and pathologic groups [9], [10]. A very recent study has implemented the first computation of the multiscale entropy for signals of the peripheral CVS (LDF signals) [11]. A nonmonotonic evolution of the multiscale entropy for LDF signals has been reported. This behavior is markedly different from the one of HRV data, displays a monotonic increase with scales. The multiscale entropy of LDF signals observed in [11] presents two distinctive scales with two extrema: the multiscale entropy first reaches a maximum and then decreases to reach a minimum. This suggests that the underlying processes present maximum and then minimum irregularities at the corresponding scales. Our goal herein is to propose both theoretical and experimental investigations to confirm the results previously reported on the multiscale entropy for LDF signals and to go forward on the understanding of the bimodal pattern observed. For this purpose, we first introduce in what follows the multiscale entropy concept. Then, based on previous spectral analyses of LDF signals where characteristic frequency bands linked to physiological

Manuscript received March 31, 2011; revised May 27, 2011; accepted June 19, 2011. Date of publication June 27, 2011; date of current version September 21, 2011. *Asterisk indicates corresponding author*.

*A. Humeau is with the Laboratoire d'Ingénierie des Systèmes Automatisés, Université d'Angers, 49000 Angers, France (e-mail: anne.humeau@univ-angers.fr).

G. Mahé and P. Abraham are with the Laboratoire de Physiologie et d'Explorations Vasculaires, UMR CNRS 6214-INSERM 771, Centre Hospitalier Universitaire d'Angers, 49033 Angers cedex 01, France (e-mail: gumahe@chu-angers.fr; piabraham@chu-angers.fr).

F. Chapeau-Blondeau and D. Rousseau are with the Laboratoire d'Ingénierie des Systèmes Automatisés, Université d'Angers, 49000 Angers, France (e-mail: chapeau@univ-angers.fr; david.rousseau@univ-angers.fr).

Color versions of one or more of the figures in this paper are available online at http://ieeexplore.ieee.org.

Digital Object Identifier 10.1109/TBME.2011.2160865

processes were reported, LDF signals are filtered to remove the spectral bands linked to some of these physiological processes. The results are analyzed, discussed, and finally interpretations for the origin of the distinctive scales observed on the multiscale entropy of LDF signals are deduced.

II. Materials and Methods

A. Measurement Procedure

Six healthy subjects (29.0 ± 6.6 years old) participated in the study. They were asked to refrain from consuming caffeine in the 2 h preceding the test and from moving during the acquisitions (to avoid outliers in the signals). A laser Doppler flowmeter was used (Perimed, Stockholm, Sweden). As suggested by the manufacturer, the time constant of the laser Doppler flowmeter was set to 0.2 s to avoid aliasing. Two LDF probes were positioned on the two forearms of each subject (one probe on each volar surface of the forearm). Two LDF signals were, thus, recorded simultaneously on each subject. The acquisitions were performed in a room with an ambient temperature set at 23 ± 1 °C, between 9.00 A.M. and 6.00 P.M. The 12 LDF signals were recorded in arbitrary units (a.u.) [12] on a computer via an A/D converter (Biopac system, Santa Barbara, CA). The sampling period T was chosen equal to 0.05 s. For each signal 23 000 samples were stored (19.16 min). These signals were then processed, as described later (no preprocessing to remove the possible outliers was performed).

B. Multiscale Entropy Analysis

Entropy is a measure of the uncertainty associated with a random variable. For a time series of n random variables $\{X_i\} = \{X_1, \ldots, X_n\}$ with set of values $\theta_1, \ldots, \theta_n$, respectively, the joint entropy is defined as $H_n = -\sum_{x_1 \in \theta_1} \cdots \sum_{x_n \in \theta_n} p(x_1, \ldots, x_n) \log(p(x_1, \ldots, x_n))$ where $p(x_1, \ldots, x_n)$ is the joint probability for the variables $X_1, \ldots, X_n$. Entropy is determined on a single-scale analysis. In order to obtain entropy values through scales, Costa *et al.* proposed the multiscale entropy concept [9], [10]. The latter consists first in constructing consecutive coarse-grained time series $\{y^{(\tau)}\}$ as $y_j^{(\tau)} = \frac{1}{\tau} \sum_{i=(j-1)\tau+1}^{j\tau} x_i, \quad 1 \le j \le N/\tau$, [9], [10] where τ is the scale factor. Then, the entropy of each coarse-grained time series is computed.

Several estimators of entropy have been described in the literature. In order to estimate entropy of experimental data (short and noisy times series), the sample entropy has been proposed [13] and used in the multiscale entropy algorithm [9], [10]. Sample entropy is the negative logarithm of the conditional probability that two patterns of length m, $x_m(i) = \{x_i, \ldots, x_{i+m-1}\}$ and $x_m(j) = \{x_j, \ldots, x_{j+m-1}\}$ for which $\mathrm{d}[x_m(i), x_m(j)] \le r$ (where $\mathrm{d}[x_m(i), x_m(j)] = \max_{k=1,\ldots,m}(|x(i+k-1) - x(j+k-1)|)$), will still verify this inequality when points x_{i+m} and x_{j+m} are added to patterns $x_m(i)$ and $x_m(j)$, respectively. More precisely, let $B_i^m(r)$ be the product of $(N-m-1)^{-1}$ by the number of template vectors $x_m(j)$ similar to $x_m(i)$ (within r) where $j = 1 \ldots N-m$ with $j \neq i$ to exclude self-matches. The average of $B_i^m(r)$ for all i is computed as

$$B^m(r) = \frac{1}{N-m} \sum_{i=1}^{N-m} B_i^m(r). \tag{1}$$

In the same way, $A_i^m(r)$ is defined as the product of $(N-m-1)^{-1}$ by the number of template vectors $x_{m+1}(j)$ similar to $x_{m+1}(i)$ (within r) where $j = 1 \ldots N-m$ with $j \neq i$. The average of $A_i^m(r)$ for all i is computed in the similar manner as in (1). $B^m(r)$ is the probability that two sequences will match for m points and $A^m(r)$ is the probability that two sequences will match for $m+1$ points. The sample entropy is then defined as $\mathrm{SampEn}(m, r) = \lim_{n \to \infty} -\ln \frac{A^m(r)}{B^m(r)}$ which is estimated by the statistic $\mathrm{SampEn}(m, r, N)$

$$\mathrm{SampEn}(m, r, N) = -\ln \frac{A^m(r)}{B^m(r)}. \tag{2}$$

Sample entropy provides a quantification of the irregularity of a temporal series. In the multiscale entropy algorithm, the sample entropy value is studied as a function of the scale factor τ [9], [10].

In our whole study, we implemented the multiscale entropy algorithm with $m = 2$ and $r = 0.15$ (as in [9]). In order to validate the results given by our implementation, we first apply the algorithm on two synthetic signals of known expression for their multiscale entropy. The first synthetic signal is a Gaussian white noise (mean: 0; variance: 1; uncorrelated noise). The second synthetic signal is a $1/f$ (long-range correlated) noise. Theoretical multiscale entropy values for white noise and $1/f$ noise can be found in [9]. For both signals, 23 000 samples are generated. Moreover, for all our LDF data, a normalization is performed before the application of the algorithm (subtraction of the mean and division by the standard deviation). In all our processes, we choose the shortest coarse-grained time series with 1000 samples (see, for example, [9]). Scale factors, therefore, go from 1 to 23.

C. Physiological Scales-Based Filtering Process

By analyzing LDF oscillations with wavelets, some authors found six spectral components within the frequency range [0.0095, 2] Hz (see, for example, [5], [14]). The physiological origins of these spectral components have been studied through different works. The authors reported that the spectral component around 1 Hz (frequency band [0.6, 2] Hz) corresponds to the cardiac activity. The spectral component in the frequency band [0.145, 0.6] Hz is related to the respiratory activity. The four other spectral components in the lowest frequency bands ([0.052, 0.145] Hz, [0.021, 0.052] Hz, [0.0095, 0.021] Hz, and [0.005, 0.0095] Hz) correspond, respectively, to the myogenic, neurogenic, nitric oxide (NO)-related endothelial, and NO-independent endothelial activities [5], [14]. Based on these findings, we filtered our LDF signals in three ways: 1) we performed a low-pass filter to remove the frequencies higher than 0.6 Hz. The cardiac activity was, therefore, suppressed from the signals; 2) a bandpass filter was applied on the original LDF time series to keep only the frequencies within the [0.6, 2] Hz band (only the cardiac activity); and 3) a high-pass

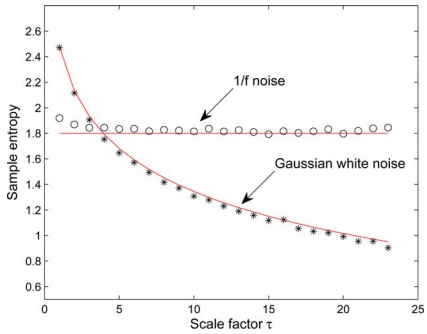

Fig. 2. Multiscale analysis of one realization of a Gaussian white noise (mean 0 and variance 1) and one realization of a $1/f$ noise. Symbols represent results of simulations and lines correspond to analytic results [9].

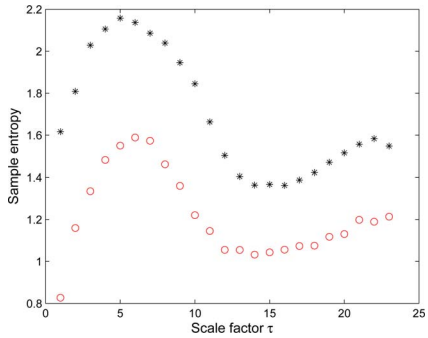

Fig. 3. Multiscale entropy values for two LDF signals recorded simultaneously on the two forearms of a healthy subject. The sampling period for the LDF signals is T = 0.05 s, which gives, for scale factors going from $\tau = 1$ to $\tau = 23$, time scales ranging from $\tau T = 0.05$ s to $\tau T = 1.15$ s.

filter was performed on the original LDF time series to keep only the frequencies higher than 2 Hz (to remove all the previously mentioned physiological activities). The filters used are Butterworth filters with an attenuation of 20 dB in the stopbands (aforementioned frequency bands where characteristic frequencies of physiological activities have been reported). On each corresponding filtered signal, the multiscale entropy was determined. The resulting values were finally compared to the ones of original LDF signals.

III. Results and Discussion

The results for the multiscale entropy of Gaussian white and $1/f$ noises are shown in Fig. 2. We note that, for the two synthetic signals, theoretical and numerically estimated multiscale entropies are close to each other for each scale factor τ studied. Moreover, we observe that the white noise possesses higher multiscale entropy values than the $1/f$ noise for scale factors below $\tau = 5$. However, the opposite is observed for scale factors larger than $\tau = 5$. This can be explained by the fact that for $1/f$ noise, the fluctuations amplitudes of the coarse-grained time series stay to high levels when the scale factor τ increases. For white noise, variance of coarse-grained time series decreases with scale factor τ. The coarse-grained time series of $1/f$ noise are therefore, in this respect, more irregular than coarse-grained time series of white noise at the corresponding scale factors.

From Fig. 3 we observe that the multiscale entropy values for representative LDF signals present a nonmonotonic behavior. Multiscale entropy increases from scale factor $\tau = 1$ to a scale factor around $\tau = 6$, where a maximum is reached. It then progressively decreases until a scale factor around $\tau = 15$, where a minimum is observed. Two distinctive scales are, therefore, identified. This nonmonotonic pattern is observed on our 12 LDF signals. The two singled out scales vary slightly between subjects, but are similar for the time series recorded simultaneously on the two forearms of each subject. LDF signals represent local microvascular blood flow and are probe-position dependent. Therefore, for a given subject, two LDF signals acquired at different locations, even if recorded simultaneously, may present different amplitude in their entropy. The results show a nonmonotonic evolution of the multiscale entropy for the 12 LDF signals. We therefore confirm the results obtained in [11] and show that the singled out scales are similar for signals recorded simultaneously at different locations on a given subject. This also shows that the observed amplitude changes in the LDF signals (amplitude changes due to physiological variations, e.g., modifications in vascular tone) do not influence much the multiscale entropy pattern. By contrast, the multiscale entropy found for HRV data increases on small time scales and then stabilizes to a constant value [10]. The nonmonotonic evolution of the multiscale entropy observed for LDF signals is, therefore, markedly different from the one of HRV data for which multiscale entropy presents a monotonic increase through scales. We note that by opposition to ECG signals from which HRV data are extracted, LDF signals do not possess any periodic pulsations. All the samples of LDF recordings are, therefore, considered in our computation.

The two distinctive scales observed show that LDF coarse-grained time series undergo specific changes from high to low irregularity: around $6T = 0.30$ s and $15T = 0.75$ s in Fig. 3. In Fig. 3, the multiscale entropy is the lowest around 0.75 s; the processes acting around this scale are, therefore, identified as having the lowest irregularity. The time scale around 0.75 s is close to the period of the heart beats. The regularity of this strong rhythmic activity could be the origin of the low multiscale entropy recorded around 0.75 s in the LDF signal. That could also explain why the singled out scales are similar for signals recorded simultaneously at different locations on a subject (central activity). In order to confirm this hypothesis, we removed one by one, with filters, the frequency bands containing the aforementioned physiological activities in order to isolate some of them. We then computed the multiscale entropy of the resulting signals (filtered signals). Representative examples of results are presented in Fig. 4. We observe that the bandpass filtered LDF signals are the ones that show a behavior with scales that is the closest to the one obtained with the original LDF signals. This is true for our 12 LDF signals. Moreover, we observe that the value of the multiscale entropy for the low-pass filtered signals increases with scales. This is also true for our 12 LDF signals. For the high-pass filtered signals, the multiscale entropy shows a decreasing pattern that reaches values near to

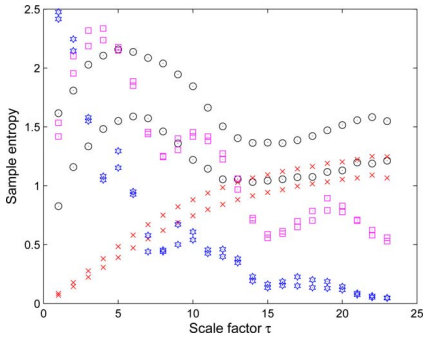

Fig. 4. Multiscale entropy values for: two LDF signals recorded simultaneously on the two forearms of a healthy subject (circles); the low-pass filtered signals (crosses); the bandpass filtered signals (squares); and the high-pass filtered signals (hexagrams). Same as in Fig. 3 for the sampling period.

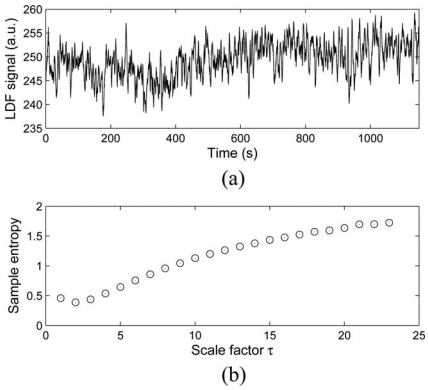

Fig. 5. (a) LDF signal recorded in a motility standard solution [12]. (b) Multiscale entropy values for the LDF signal presented in (a). Same as in Fig. 3 for the sampling period.

0 for the highest scales studied. This is also true for our 12 LDF signals.

From these results, we can suggest that the pattern of the multiscale entropy observed for LDF signals on scales ranging from 0 to 1.15 s is probably of central origin and probably mainly due to the activities acting in the scale range [0.5, 1.66] s (frequency band [0.6, 2] Hz). The heart rate being in this range of scales and being a central activity, we can hypothesize that the pattern of the multiscale entropy for LDF signals may be dominated by the regularity of the heart beats. The other physiological activities (in the frequency range lower than 0.6 Hz) lead to growing multiscale entropy values with scales (see Fig. 4). This behavior is also the one recorded in a solution of polystyrene particles dispersed in water where a Brownian motion can be hypothesized (motility standard solution [12]) for the underlying physical process producing the backscattered light, and resulting in a measured LDF signal which is analyzed in Fig. 5. The high-pass filtered signals present a multiscale entropy with a decreasing pattern that reaches values near to 0 for the highest scales studied. This decreasing behavior is close to the one observed with Gaussian white noise (see Fig. 2). These findings may be due to the role played by low frequencies in the entropy at large scales. Further work is needed to explain these latter behaviors.

IV. Conclusion

Multiscale entropy analysis is herein proposed to quantify the irregularity of microvascular blood flow signals. The multiscale entropy of LDF signals shows a nonmonotonic behavior. This is markedly different from the results found for HRV data where multiscale entropy increases with scales. Multiscale entropy of LDF signals presents two distinctive scales where LDF signals undergo specific changes from high to low irregularity. These two distinctive scales are similar for signals recorded simultaneously at different locations on a given subject, suggesting the implication of a common central activity. These results with the ones given by physiological scales-based filtered signals complement previous ones (e.g., [15]) and provide ground to support that the behavior of the multiscale entropy for LDF signals is dominated by the cardiac activity.

References

[1] G. E. Nilsson, T. Tenland, and P. A. Oberg, "Evaluation of a laser Doppler flowmeter for measurement of tissue blood flow," *IEEE Trans. Biomed. Eng.*, vol. BME-27, no. 10, pp. 597–604, Oct. 1980.

[2] G. E. Nilsson, T. Tenland, and P. A. Oberg, "A new instrument for continuous measurement of tissue blood flow by light beating spectroscopy," *IEEE Trans. Biomed. Eng.*, vol. BME-27, no. 1, pp. 12–19, Jan. 1980.

[3] A. Humeau, B. Buard, G. Mahé, F. Chapeau-Blondeau, D. Rousseau, and P. Abraham, "Multifractal analysis of heart rate variability and laser Doppler flowmetry fluctuations: Comparison of results from different numerical methods," *Phys. Med. Biol.*, vol. 55, pp. 6279–6297, 2010.

[4] S. Assous, A. Humeau, M. Tartas, P. Abraham, and J. P. L'Huillier, "S-transform applied to laser Doppler flowmetry reactive hyperemia signals," *IEEE Trans. Biomed. Eng.*, vol. 53, no. 6, pp. 1032–1037, Jun. 2006.

[5] A. Stefanovska, M. Bracic, and H. D. Kvernmo, "Wavelet analysis of oscillations in the peripheral blood circulation measured by laser Doppler technique," *IEEE Trans. Biomed. Eng.*, vol. 46, no. 10, pp. 1230–1239, Oct. 1999.

[6] J. Hu, J. Gao, W. W. Tung, and Y. Cao, "Multiscale analysis of heart rate variability: A comparison of different complexity measures," *Ann. Biomed. Eng.*, vol. 38, pp. 854–864, 2010.

[7] E. S. C. Ching and Y. K. Tsang, "Multifractality and scale invariance in human heartbeat dynamics," *Phys. Rev. E*, vol. 76, 041910, 2007.

[8] P. Ch. Ivanov, L. A. N. Amaral, A. L. Goldberger, S. Havlin, M. G. Rosenblum, Z. R. Struzik, and H. E. Stanley, "Multifractality in human heartbeat dynamics," *Nature*, vol. 399, pp. 461–465, 1999.

[9] M. Costa, A. L. Goldberger, and C. K. Peng, "Multiscale entropy analysis of biological signals," *Phys. Rev. E*, vol. 71, 021906, 2005.

[10] M. Costa, A. L. Goldberger, and C. K. Peng, "Multiscale entropy analysis of complex physiologic time series," *Phys. Rev. Lett.*, vol. 89, 068102, 2002.

[11] A. Humeau, B. Buard, G. Mahé, D. Rousseau, F. Chapeau-Blondeau, and P. Abraham, "Multiscale entropy of laser Doppler flowmetry signals in healthy subjects," *Med. Phys.*, vol. 37, pp. 6142–6146, 2010.

[12] *PeriFlux System 5000 Extended User Manual,* PeriMed, Stockholm Sweden, 2006.

[13] J. S. Richman and J. R. Moorman, "Physiological time-series analysis using approximate entropy and sample entropy," *Amer. J. Physiol. Heart Circ. Physiol.*, vol. 278, pp. H2039–H2049, 2000.

[14] P. Kvandal, S. A. Landsverk, A. Bernjak, A. Stefanovska, H. D. Kvernmo, and K. A. Kirkeboen, "Low-frequency oscillations of the laser Doppler perfusion signal in human skin," *Microvasc. Res.*, vol. 72, pp. 120–127, 2006.

[15] Y. Shiogai, A. Stefanovska, and P. V. E. McClintock, "Nonlinear dynamics of cardiovascular ageing," *Phys. Rep.*, vol. 488, pp. 51–110, 2010.